Multiantenna Wireless Architectures with Low Precision Converters

YASAMAN ETTEFAGH

Multiantenna Wireless Architectures with Low Precision Converters

Yasaman Ettefagh

This thesis has been prepared using LaTeX.

To my family

Abstract

One of the main key technology enablers of the next generation of wireless communications is massive multiple input multiple output (MIMO), in which the number of antennas at the base station (BS) is scaled up to the order of tens or hundreds. It provides considerable energy and spectral efficiency by spatial multiplexing, which enables serving multiple user equipments (UEs) on the same time and frequency resource. However, the deployment of such large-scale systems could be challenging and this thesis is aimed at studying one of the challenges in the optimal implementation of such systems. More specifically, we consider a fully digital setup, in which each antenna at the BS is connected to a pair of data converters through a radio-frequency (RF) chain, all located at the remote radio head (RRH), and there is a limitation on the capacity of the fronthaul link, which connects the RRH to the baseband unit (BBU), where digital signal processing is performed. The fronthaul capacity limitation calls for a trade-off between some of the design parameters, including the number of antennas, the resolution of data converters and the over-sampling ratio. In this thesis, we study the aforementioned trade-off considering the first two design parameters.

First, we consider a quasi-static scenario, in which the fading coefficients do not change throughout the transmission of a codeword. The channel state information (CSI) is assumed to be unknown at the BS, and it is acquired through pilot transmission. We develop a framework based on the mismatched decoding rule to find lower bounds on the achievable rates. The bi-directional rate at 10% outage probability is selected as the performance metric to determine the recommended architecture in terms of number of antennas and the resolution of data converters.

Second, we adapt our framework to a finite blocklength regime, considering a realistic mm-wave multi-user clustered MIMO channel model and a well suited channel estimation algorithm. We start our derivations by considering random coding union bound with parameter s (RCUs) and apply approximations to derive the corresponding normal approximation and further, an easy to compute outage with correction bound. We illustrate the accuracy of our approximations, and use the outage with correction bound to investigate the optimal architecture in terms of the number of antennas and the resolution of the data converters.

Our result show that at low signal to noise (SNR) regime, we benefit from lowering the resolution of the data converters and increasing the number of antennas, while at high SNR for a practical scenario, the optimal architecture could move to 3 or 4 bits of resolution since we are not in demand of large array gain anymore.

Keywords: massive MIMO, data converters, fronthaul link, outage probability, random coding union bound with parameter s, normal approximation

List of Publications

This thesis is based on the following publications:

[A] **Y. Ettefagh**, S. Jacobsson, A. Hu, G. Durisi, and C. Studer, "All-digital massive MIMO uplink and donlink rates under a fronthaul constraint" in *Proc. Asilomar Conf. Signals, Syst., Comput.,*, Pacific Grove, CA, USA, Nov. 2019, pp 416-420.

[B] **Y. Ettefagh**, S. R. Aghdam, G. Durisi, S. Jacobsson, M. Coldrey, and C. Studer, "Performance of Quantized Massive MIMO with Fronthaul Rate Constraint over Quasi-Static Channels", To be submitted to *IEEE Transactions on Wireless Communications*.

Other publications by the author, not included in this thesis, are:

[C] S. Jacobsson, **Y. Ettefagh**, G. Durisi, and C. Studer, "All-digital massive MIMO with a fronthaul constraint" in *Proc. IEEE Statistical Sig. Pro. Workshop*, Freiburg, Germany, Jun. 2018.

Acknowledgments

Acronyms

IoT:	Internet of Things
FWA:	fixed wireless access
MIMO:	multiple-input multiple-output
RF:	radio frequency
BBU:	baseband unit
RRH:	remote radio head
BS:	base station
UE:	user equipment
ADC:	analog to digital converter
DAC:	digital to analog converter
LMMSE:	linear minimum mean square error
SNR:	signal to noise ratio
TDD:	time division duplex
CSI:	channel state information
MU:	multi-user
NMSE:	normalized mean square error
MF:	matched-filtering
ZF:	zero-forcing
MMSE:	minimum mean square error
MUI:	multi-user interference
SINR:	signal to interference plus noise ratio
DA-MMSE:	distortion-aware minimum mean square error

Contents

Part I

Overview

Introduction

1.1 Overview

In the modern society, the application of telecommunications is not limited to making audio/video calls anymore. In fact, the areas in which telecommunications play a role are far beyond one could have imagined a few decades ago. Its impacts on business, education, marketing, health such as the recent pandemic, etc., are crucial. The current networked society demands ubiquitous connectivity and the number of active nodes in the whole network is scaled by the number of smart gadgets that we want to connect to the network. With the advancements in Internet of Things (IoT), this need is even more pronounced. As a comparison, the predicted global mobile data traffic excluding fixed wireless access (FWA) for 2021 was 51EB/m (exhabytes per month) and the actual total mobile traffic was estimated 65EB/m at the end of 2021. Furthermore, the total mobile traffic is predicted to be 288EB/m in 2027 [1]. To realize such a considerable requirement, we need to provide enabling technologies. Fig. 1.1 shows the trend of global mobile network data traffic and the contribution of 5G, previous generations as well as FWA.

Wireless communication is an evolving technology, introducing a new generation approximately every decade. Considering the ever-increasing demands due to new use cases and requirements, enabling technologies are invented and developed to meet the requirements. [2, 3]

Massive multiple-input-multiple-output (MIMO) is one of the key technologies to realize the requirements of 5G and beyond [4, 5]. By leveraging a large number of antennas at the base station (BS) and using finely tuned beamforming techniques, many user equip-
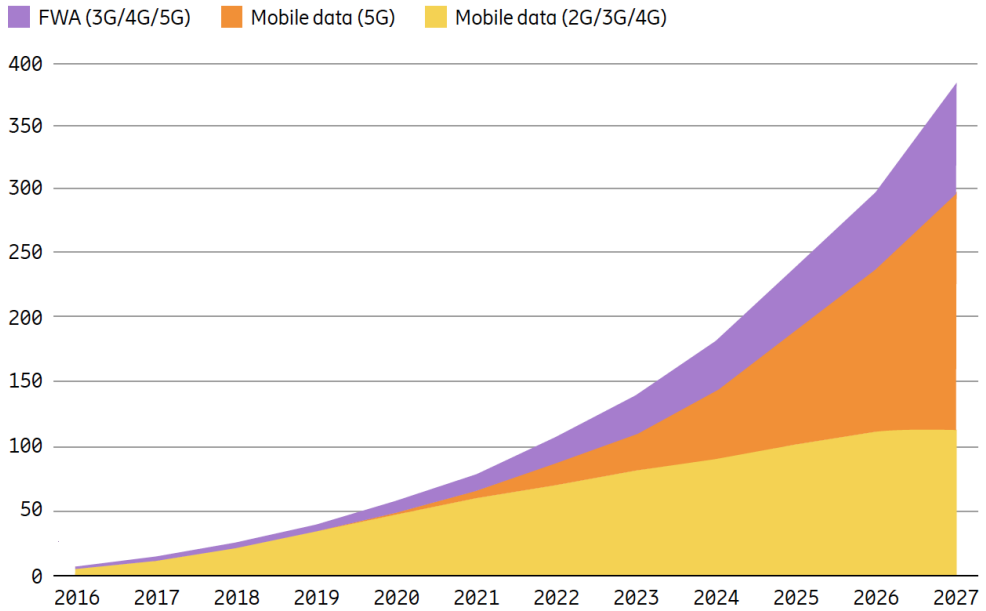
Figure 1.1: Global mobile network data traffic (EB per month) [1]

ments (UEs) can be served via spatial multiplexing on the same time and frequency resource. Therefore, noticeable gains in terms of spectral and energy efficiency can be achieved [26].

Two different architectures have been proposed and studied to realize massive MIMO networks. Fully digital architectures, in which each antenna is connected to an individual radio frequency (RF) circuitry containing mixers, power amplifiers, etc., and a pair of data converters, and hybrid architectures in which with the beamforming is implemented by combining digital processing and a network of phase shifters. Fully digital architectures yield significant throughput, full flexibility and do not need antenna calibration. Therefore they are more attractive and in this thesis, we will focus on all-digital architectures.

Despite the advantages of a fully digital massive MIMO setup, equipping the BS with a large number of antennas comes with a cost in the implementation. In a conventional setup with high resolution data converters, the total power consumption is large since high-resolution data converters are power hungry devices [7]. Therefore, using low-resolution data converters is a key solution to reduce the power consumption. The drawback of using low-resolution data converters is the nonlinear distortion they cause to their input signal. The performance of massive MIMO with low-resolution data converters, have been extensively studied in the literature, and it is shown that, despite

the impairments these nonlinear devices bring about, with the help of enough antennas and depending on the number of UEs, it is possible to approach the performance of the infinite-resolution setup by using only a few bit-resolution data converters. [4, 7, 10, 11]

Another drawback of a fully digital architecture is related to the capacity limitations of the fronthaul link. In some deployments, the remote radio head (RRH) containing the antennas and the RF chains is separated from the baseband unit (BBU). The link connecting these two units is called the fronthaul link and has a limited capacity. Using high resolution data converters in the context of massive MIMO and mm-wave communication can easily end up in few terabytes per second of raw data to be transferred through this link. Therefore, by lowering the resolution of data converters, it is possible to limit the required fronthaul data rate.

This thesis is aimed at providing an analytical framework to assess the tradeoff between different realizations of such systems in terms of number of antennas and resolution of data converters when there is a constraint on the capacity of the fronthaul link. We considered practically relevant scenarios to make our analyses close to the reality as much as possible.

1.2 Thesis Outline

Part I of this thesis is organized as follows. In Chapter 2, data converters are introduced and an analytical tool to simplify the derivations is reviewed. In Chapter 3, we provide a review of the quantized multi-user (MU) massive MIMO setup and describe a well-known channel model that is frequently used in practice in the context of mm-wave communications. Chapter 4 contains a summary of the appended papers appearing in Part II.

1.3 Notation

Lowercase and uppercase boldface letters and lowercase letters denote column vectors, matrices and scalars, respectively. The set of real numbers and complex numbers are indicated by $\mathbb{R}$ and $\mathbb{C}$ respectively. For a matrix A, its complex conjugate, transpose, and Hermitian transpose are denoted A^*, A^{T}, and A^{H}, respectively. The operators $\mathbb{E}$ and $\mathrm{diag}(\mathbf{B})$ denotes the mathematical expectation over the specified random variable and the diagonal elements of a square matrix $\mathbf{B}$. An all-zero vector of dimension N is denoted by $\mathbf{0}_N$. The complex-valued N-dim circularly-symmetric Gaussian probability density function with zero mean and covariance $\mathbf{K}$ is shown by $\mathcal{CN}(\mathbf{0}_N, \mathbf{K})$. The real and imaginary parts of a signal are indicated by $\Re(.)$ and $\Im(.)$.

Data Converters

In a practical communication system, data converters are required to convert signals from analog to digital domain and vise versa. More specifically, in uplink, ADCs are used to convert the received analog signal at the base station to digital signal so that the data can be processed digitally at the base-band unit. In downlink, DACs are leveraged to convert the digital signal to analog signal so that it can be transmitted on the wireless channel. In this thesis, the users are assumed to be equipped with infinite-resolution data converters, and the BS is assumed to be equipped with low-resolution data converters. The power consumption of data converters scales exponentially with their resolution [7]. Data converters are non-linear devices that cause irreversible distortion to the input signal which is increased by lowering the resolution. In this chapter, we review a mathematical tool that is used to linearlize the effect of data converters, which facilitates the derivations. Moreover, we review a phenomenon called stochastic resonance that happens in the case of single-bit resolution data converters at high signal to noise ratio (SNR).

2.1 Linearization using Bussgang Theorem

As mentioned earlier, data converters are non-linear devices. In this thesis, uniform, symmetric, mid-rise quantizers are considered. Considering the input to be $r \in \mathbb{R}$, the quantizer signal $\mathcal{Q}(r)$ is given by

$$y = \mathcal{Q}(r) = \begin{cases} \frac{\Delta}{2}(1 - 2^Q) & \text{if } r < -\frac{\Delta}{2}2^Q \\ \Delta\lfloor \frac{r}{\Delta} \rfloor + \frac{\Delta}{2} & \text{if } -\frac{\Delta}{2}2^Q < r < \frac{\Delta}{2}2^Q \\ \frac{\Delta}{2}(2^Q - 1) & \text{if } r \geq \frac{\Delta}{2}2^Q. \end{cases} \tag{2.1}$$

Here, Q and Δ are the resolution and step size of the quantizer respectively. To keep the notation compact, the quantization labels are represented by the set $\mathcal{L} = \{l_0, ..., l_{L-1}\}$ where $L = 2^Q$ denotes the number of quantization levels and the quantization thresholds are characterized by the set $\mathcal{T} = \{\tau_0, ..., \tau_L\}$ where $\tau_0 = -\infty$ and $\tau_L = +\infty$. We consider complex random vector by taking $\mathbf{z} \in \mathcal{C}^n$ to be the input and a pair of quantizers each for the real and the imaginary part, separately. In order to linearize the input/output relation, we can write the quantized signal as the summation of the linear minimum mean square error (LMMSE) estimate of the input plus an uncorrelated distortion. In case of $\mathbf{z}$ being Gaussian distributed, it is possible to use a mathematical tool called Bussgang theorem [23] and the LMMSE takes a simple form as below.

Theorem 1: *The cross-correlation of two Gaussian signals, when one of them has undergone a non-linear transformation, is the same as the cross-correlation of them before the non-linear transformation except for a scaling factor called Bussgang gain.*

As a result of Bussgang theorem, we can write the linearized input/output relation of $\mathbf{y} = \mathcal{Q}(\mathbf{z})$, where $\mathbf{z} \sim \mathcal{CN}(\mathbf{0}, \mathbf{C_z})$ as below:

$$\mathbf{y} = \mathbf{Gz} + \mathbf{d}, \tag{2.2}$$
$$\mathbf{G} = \mathbb{E}\left[\mathcal{Q}(\mathbf{z})\mathbf{z}^{\mathrm{H}}\right]\mathbb{E}\left[\mathbf{zz}^{\mathrm{H}}\right]^{-1} = \mathbf{C_{yz}}\mathbf{C_z}^{-1}.$$

Here, $\mathbf{C_{yz}} = \mathbb{E}[\mathbf{yz}^{\mathrm{H}}]$ denotes the covariance between $\mathbf{y}$ and $\mathbf{z}$. The distortion $\mathbf{d}$ is a non-Gaussian and zero-mean random vector uncorrelated to both $\mathbf{z}$ and $\mathbf{y}$. The covariance matrix of $\mathbf{d}$ turns out to be useful in further analyses related to achievable rates. For the case of mid-rise quantizer function (2.1), the Bussgang matrix is given by [4, 10]

$$\mathbf{G} = \frac{\Delta}{\sqrt{\pi}}\mathrm{diag}(\mathbf{C_z})^{-1/2} \sum_{i=1}^{L-1} \exp\left(-\frac{\Delta^2}{2}(i - L/2)^2 \mathrm{diag}(\mathbf{C_z})^{-1}\right). \tag{2.3}$$

2.2 Covariance Matrix of Distortion

According to (2.2), the covariance matrix of distortion has the following form:

$$\mathbf{C_d} = \mathbb{E}\left[(\mathbf{y} - \mathbf{Gz})(\mathbf{y} - \mathbf{Gz})^{\mathrm{H}}\right] = \mathbf{C_y} - \mathbf{GC_zG}. \tag{2.4}$$

Note that since $\mathbf{G}$ is a real diagonal matrix, $\mathbf{G}^{\mathrm{H}} = \mathbf{G}$. To evaluate $\mathbf{C_d}$, we need to find the covariance of the quantized signal $\mathbf{y}$. It holds that

$$[\mathbf{C_y}]_{p,q} = \mathbb{E}[y_p y_q^*] = 2\left(\mathbb{E}[y_p^R y_q^R] + j\mathbb{E}[y_p^I y_q^R]\right), \qquad p, q = 1, .., n. \tag{2.5}$$

where $y_p^R = \Re\{y_p\}$ and $y_p^I = \Im\{y_p\}$. For the case of $p = q$, $\mathbb{E}[y_p^I y_q^R] = 0$, therefore, the (p, p) elements of $\mathbf{C_y}$ can be derived as [14]

$$[\mathbf{C_y}]_{p,p} = 2\mathbb{E}[y_p^R y_p^R] = 2\sum_{i=0}^{L-1} l_i{}^2 \mathbb{P}[y_p^R = l_i] \tag{2.6}$$

$$= 2\sum_{i=0}^{L-1} l_i^2 \mathbb{P}[\tau_i \le z_p^R < \tau_{i+1}] \tag{2.7}$$

$$= 2\sum_{i=0}^{L-1} l_i{}^2 \left(\Phi\left(\frac{\sqrt{2}\tau_{i+1}}{\sigma_p} \right) - \Phi\left(\frac{\sqrt{2}\tau_i}{\sigma_p} \right) \right) \tag{2.8}$$

$$= \frac{\Delta^2}{2}(L-1)^2 - 4\Delta^2 \sum_{i=1}^{L-1} \left(i - \frac{L}{2} \right) \Phi\left(\frac{\sqrt{2}}{\sigma_p} \left(i - \frac{L}{2} \right) \right). \tag{2.9}$$

Here, $\sigma_p = [\mathbf{C_z}]_{p,p}^{1/2}$ and $\Phi(x) = \sqrt{1/2\pi} \int_{-\infty}^{x} e^{-t^2/2} dt$ is the cumulative distribution function of the standard normal random variable. There is no closed-form expression for the off-diagonal elements of $\mathbf{C_y}$ available for $Q > 1$. For the case of 1-bit data converters, the covariance matrix can be expressed in closed-form using the arcsine law as below [15]

$$\mathbf{C_y} = \frac{2}{\pi} \left[\arcsin\left(\text{diag}(\mathbf{C_z})^{-\frac{1}{2}} \mathbf{C_z} \text{diag}(\mathbf{C_z})^{-\frac{1}{2}} \right) \right]. \tag{2.10}$$

For $Q > 1$, there are approximations proposed in the literature such as the diagonal approximation [14]. This approximation is based on the observation that the diagonal elements of $\mathbf{C_y}$ can be computed exactly [14]. By modeling the distortion caused by quantizers as a white process, the off-diagonal elements of distortion matrix are assumed to be zero. Therefore, $\mathbf{C_d}$ can be approximated as below

$$\mathbf{C_d^{\text{diag}}} = \text{diag}\left(\mathbf{C_y} \right) - \mathbf{G} \text{diag}\left(\mathbf{C_z} \right) \mathbf{G}^{\text{H}} \tag{2.11}$$

$$= \frac{\Delta^2}{2}(L-1)^2 \mathbf{I}_n - 4\Delta^2 \sum_{i=1}^{L-1} (i - L/2) \Phi\left(\sqrt{2}\,(i - L/2) \text{diag}\left(\mathbf{C_z} \right)^{-1/2} \right).$$

In Chapter 3, some numerical results to show the accuracy of the diagonal approximation are illustrated.

2.3 Stochastic Resonance and Dithering for 1-Bit ADCs

Single-bit resolution ADCs are in fact comparators, and they do not preserve the amplitude information of the input signal, meaning that the outputs of $\mathcal{Q}(r)$ and $\mathcal{Q}(\alpha r)$, $\alpha > 0$ are the same in case of 1-bit quantizers. Now suppose that noisy observations are available to be quantized. For low and medium signal SNR values, the additive noise turns out to be useful since it changes the output of the quantization. Therefore,

in case of having multiple noisy observations of the desired signal, we can recover the amplitude of the desired signal to some extent. This phenomenon is called stochastic resonance [16, 34]. In the case of high SNR, this phenomenon does not happen anymore, since the additive noise term can be neglected and does not contribute to the output of the quantization. Therefore, 1-bit ADCs suffer from loss of amplitude information in high SNR. In such a case, it is possible to add more noise to synthetically reduce the SNR operating point. This process is called dithering and is being used to improve the performance of 1-bit data converters [18, 19]. For this reason, we have used dithering at high SNR regime in Paper B.

CHAPTER 3

Multi-user Massive MIMO

The purpose of this chapter is to take a look at how lower bounds on the uplink and downlink achievable rates are derived in an all-digital low-resolution multi-user (MU) massive MIMO setup. In this thesis, a single cell is considered in which a BS with B antennas communicates with $U \ll B$ single antenna UEs on the same time and frequency resource with the help of spatial multiplexing as shown in Fig 3.1. The antennas at the BS are connected to a pair of data converters that quantize the real and imaginary parts of the input signal separately. The wireless channel is denoted by $\mathbf{H}^{B \times U}$ and is modeled as a block-fading channel, i.e., it remains constant throughout the transmission of a codeword.

In practice, the BS and UEs do not have the knowledge of the channel state information (CSI) and the channel needs to be estimated. We assume that the system operates in time division duplex (TDD) mode, meaning that the uplink and downlink operate on the same frequencies but in different time intervals. With this assumption, the estimated channel on the uplink can be used in the downlink as well. In this chapter, in order to put our focus on derivations of the lower bounds on the achievable rates, the BS and UEs are assumed to have the full knowledge of CSI. This assumption is relaxed in Paper A and B. Moreover, we discuss the derivations of commonly used ergodic capacity in this thesis, while we switch to the outage capacity in Paper A and B which is more appropriate for the case of short packet transmission. Finally, we illustrate the lower bounds on the achievable rates using the channel model that was used in Paper B.
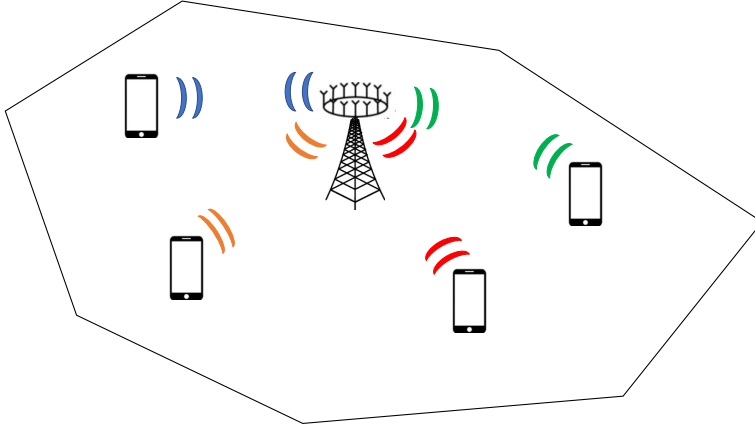
Figure 3.1: A single cell scenario in which a *B*-antenna BS serves *U* UEs on the same time and frequency resource.

3.1 Uplink Transmission

In the uplink, U UEs transmit signals to the BS. The received signal $\mathbf{y}^{\text{ul}} \in \mathcal{C}^B$ at the BS at time instant k can be written as

$$\mathbf{y}_k^{\text{ul}} = \sqrt{\rho^{\text{ul}}}\mathbf{H}\mathbf{s}_k^{\text{ul}} + \mathbf{n}_k^{\text{ul}}, \tag{3.1}$$

where $\mathbf{n}_k^{\text{ul}} \sim \mathcal{CN}(\mathbf{0}_B, \mathbf{I}_B)$ is the additive noise and the transmit signal vector is $\mathbf{s}_k^{\text{ul}} = [s_{k,1}^{\text{ul}}, ..., s_{k,U}^{\text{ul}}] \in \mathcal{C}^U$. The signals $s_{k,u}^{\text{ul}}, u = 1, ..., U$ are drawn independently from $\mathcal{CN}(0, 1)$ and ρ^{ul} is the uplink SNR. The received signal $\mathbf{y}_k^{\text{ul}}$ passes through an automatic gain controller circuit (AGC) and a pair of Q-bit quantizers at each antenna. The purpose of the AGC circuit is to set the dynamic range of the input signal to the quantizer such that the probability of overload does not exceed a certain range. The resultant quantized signal is

$$\mathbf{r}_k^{\text{ul}} = \mathcal{Q}(\mathbf{A}(\sqrt{\rho^{\text{ul}}}\mathbf{H}\mathbf{s}_k^{\text{ul}} + \mathbf{n}_k^{\text{ul}})), \tag{3.2}$$

where $\mathbf{A}$ models the AGC circuit and $\mathcal{Q}(.)$ is the quantizer function given in (2.1). Following the derivations of Bussgang linearization in Section 2.1, (3.2) can be written as

$$\mathbf{r}_k^{\text{ul}} = \mathbf{G}^{\text{ul}}\mathbf{A}(\sqrt{\rho^{\text{ul}}}\mathbf{H}\mathbf{s}_k^{\text{ul}} + \mathbf{n}_k^{\text{ul}}) + \mathbf{d}_k^{\text{ul}}, \tag{3.3}$$

Here, $\mathbf{G}^{\mathrm{ul}}$ is the Bussgang matrix (2.3) and $\mathbf{d}^{\mathrm{ul}}$ is a non-Gaussian quantization noise that is uncorrelated to $\mathbf{y}^{\mathrm{ul}}$ and its covariance $\mathbf{C}_{\mathbf{d}}^{\mathrm{ul}}$ can be found by arcsine law in case of $Q = 1$ or approximated for $Q > 1$ as explained in Section 2.2, in which the covariance of the input to the quantizer $\mathbf{z}_k^{\mathrm{ul}} = \mathbf{A}\mathbf{y}_k^{\mathrm{ul}}$ is $\mathbf{C}_{\mathbf{z}}^{\mathrm{ul}} = \mathbf{A}\mathbf{C}_{\mathbf{y}}^{\mathrm{ul}}\mathbf{A}$.

In this thesis, we make use of sub-optimal linear processing at the BS because of its simplicity. In case of large number of BS antennas, linear processing turns out to be near optimal under favorable propagation [4], [20]. The idea of linear processing in uplink is to find a matrix $\mathbf{W}$ which we refer to as the combiner matrix, and multiply it by the received signal such that an estimate of each users's stream is obtained, as below

$$\hat{\mathbf{s}}_k^{\mathrm{ul}} = \mathbf{W}^{\mathrm{H}}\mathbf{r}_k^{\mathrm{ul}} = \mathbf{W}^{\mathrm{H}}\left(\mathbf{G}^{\mathrm{ul}}\mathbf{A}(\sqrt{\rho^{\mathrm{ul}}}\mathbf{H}\mathbf{s}_k^{\mathrm{ul}} + \mathbf{n}_k^{\mathrm{ul}}) + \mathbf{d}_k^{\mathrm{ul}}\right). \tag{3.4}$$

The ergodic sum-rate is lower bounded by

$$R_{\mathrm{sum}}^{\mathrm{ul}} = \mathbb{E}_{\mathbf{H}}\left[\sum_{u=1}^{U}\log(1 + \gamma_u^{\mathrm{ul}})\right], \tag{3.5}$$

where γ_u^{ul} is the received signal to noise plus distortion plus interference ratio (SINDR) at the uth UE, given by

$$\gamma_u^{\mathrm{ul}} = \frac{\rho^{\mathrm{ul}}|\mathbf{w}_u^{\mathrm{H}}\mathbf{G}^{\mathrm{ul}}\mathbf{A}\mathbf{h}_u|^2}{\rho^{\mathrm{ul}}\sum_{v\neq u}|\mathbf{w}_u^{\mathrm{H}}\mathbf{G}^{\mathrm{ul}}\mathbf{A}\mathbf{h}_v|^2 + \mathbf{w}_u^{\mathrm{H}}\mathbf{C}_{\mathbf{d}}^{\mathrm{ul}}\mathbf{w}_u + ||\mathbf{A}\mathbf{G}^{\mathrm{ul}}\mathbf{w}_u||^2} \tag{3.6}$$

This lower bound is found by treating the residual multi-user interference (MUI) and the quantization noise as an independent Gaussian noise to reflect the worst-case scenario [22, App B] and is achieved by Gaussian signaling.

Three well-known linear combiners are matched-filtering (MF), zero-forcing (ZF) and minimum mean square error (MMSE). The idea of MF is to maximize the per-user SNR, and its main drawback is that it does not consider MUI. Therefore, the performance of MF combiner is satisfactory at low SNR regime whereas it does not perform well at high SNR regime. ZF combiner on the other hand, eliminates the MUI by putting nulls in the directions of the non-intended users, but it does not take into account AWGN. Therefore, it works well at high SNR regime and poorly at low SNR regime because of noise enhancement. The purpose of the MMSE combiner is to minimize the mean-square error between the estimate $\hat{\mathbf{s}}$ and $\mathbf{s}$. It also maximizes the received SINR, therefore it outperforms ZF and MF combiners. The classical MF, ZF and MMSE combiners do not take into account the effect of quantization distortion. In [22] and [6], distortion-aware (DA) version of MMSE combiner has been introduced which maximizes the received SINDR. The ZF, MF and DA-MMSE combiners are defined as below.

$$\mathbf{W} = \begin{cases} \mathbf{G}^{\mathrm{ul}}\mathbf{A}\mathbf{H} & \text{for MF,} \\ \left(\mathbf{G}^{\mathrm{ul}}\mathbf{A}\mathbf{H}\right)\left(\left(\mathbf{G}^{\mathrm{ul}}\mathbf{A}\mathbf{H}\right)^{\mathrm{H}}\mathbf{G}^{\mathrm{ul}}\mathbf{A}\mathbf{H}\right)^{-1} & \text{for ZF,} \end{cases}$$

and for DA-MMSE combiner we have [6]

$$\mathbf{w}_u = \left(\rho^{\mathrm{ul}} \left(\sum_{v \neq u} \mathbf{G}^{\mathrm{ul}} \mathbf{A} \mathbf{h}_v \left(\mathbf{G}^{\mathrm{ul}} \mathbf{A} \mathbf{h}_v \right)^{\mathrm{H}} \right) + \mathbf{G}^{\mathrm{ul}} \mathbf{A} (\mathbf{G}^{\mathrm{ul}} \mathbf{A})^{\mathrm{H}} + \mathbf{C}_{\mathrm{d}}^{\mathrm{ul}} \right)^{-1} \tag{3.7}$$

$$\times \left(\rho^{\mathrm{ul}} \mathbf{G}^{\mathrm{ul}} \mathbf{A} \mathbf{h}_u \right), \tag{3.8}$$

where $\mathbf{w}_u, u = 1, ..., U$ are columns of the combiner matrix $\mathbf{W}$. In Paper B, we proceed with DA-MMSE combiner.

3.2 Downlink Transmission

The U-dimensional discrete-time received signal at time instant k at U UEs can be written as

$$\mathbf{y}_k^{\mathrm{dl}} = \mathbf{H}^{\mathrm{T}} \alpha \mathcal{Q} \left(\mathbf{z}_k^{\mathrm{dl}} \right) + \mathbf{n}_k^{\mathrm{dl}}, \tag{3.9}$$

where $\mathcal{Q}(.)$ denotes the quantizer function given in (2.1). The vector $\mathbf{n}_k^{\mathrm{dl}} \sim \mathcal{CN}(\mathbf{0}_U, \mathbf{I}_U)$ represents the AWGN at the UEs' side and the transmit signal is shown by $\mathbf{z}_k^{\mathrm{dl}}$. The factor α is a power-normalization factor to satisfy the transmit power constraint of ρ^{dl} which is set by treating the input to the quantizer as a complex Gaussian random variable as below

$$\alpha = \frac{\sqrt{\rho^{\mathrm{dl}}/2}}{\sqrt{\sum_{i=0}^{L-1} l_i^2 \left(Q(\sqrt{2}\tau_i) - Q(\sqrt{2}\tau_{i+1}) \right)}}. \tag{3.10}$$

Here, $Q(x) = \sqrt{1/2\pi} \int_x^\infty e^{-t^2/2} dt$ denotes the Q-function. Similar to the uplink, we use linear processing for downlink as well. The signals intended to UEs are shown by $\mathbf{s}_k^{\mathrm{dl}} = [s_{1,k}^{\mathrm{dl}}, ..., s_{U,k}^{\mathrm{dl}}] \in \mathcal{C}^U$ where $\mathbb{E}[|s_{u,k}^{\mathrm{dl}}|^2] = 1$ for $u = 1, ..., U$ are mapped to $\mathbf{z}_k^{\mathrm{dl}}$ to be transmitted through the downlink channel $\mathbf{H}^{\mathrm{T}}$ using the precoding matrix $\mathbf{P}$ as below

$$\mathbf{z}_k^{\mathrm{dl}} = \mathbf{P} \mathbf{s}_k^{\mathrm{dl}}. \tag{3.11}$$

The purpose of using precoders is to form the (unquantized) transmitted signal $\mathbf{z}_k^{\mathrm{dl}}$ such that no heavy processing is required at UE sides to obtain a soft estimate $\hat{\mathbf{s}}_k^{\mathrm{dl}}$. Three conventional precoders are ZF, MF and MMSE. These precoders are dual versions of the corresponding combiners with the same objectives and properties. Assuming a non-quantized setup, these precoders are formulated as below

$$\mathbf{P} = \begin{cases} \beta \mathbf{H}^* & \text{for MF}, \\ \beta \mathbf{H}^* \left(\mathbf{H}^{\mathrm{T}} \mathbf{H}^* \right)^{-1} & \text{for ZF}, \\ \beta \mathbf{H}^* \left(\mathbf{H}^{\mathrm{T}} \mathbf{H}^* + \frac{U}{\rho^{\mathrm{dl}}} \mathbf{I}_U \right)^{-1} & \text{for MMSE}. \end{cases}$$

Here, the factor β is chosen such that $\mathbb{E}[||\mathbf{Ps}_k^{\mathrm{dl}}||^2] = B$.

Similar to the uplink case, using Bussgang linearization (2.2), (3.9) can be written as

$$\mathbf{y}_k^{\mathrm{dl}} = \mathbf{H}^{\mathrm{T}}\mathbf{G}^{\mathrm{dl}}\left(\mathbf{Ps}_k^{\mathrm{dl}}\right) + \mathbf{H}^{\mathrm{T}}\mathbf{d}_k^{\mathrm{dl}} + \mathbf{n}_k^{\mathrm{dl}}. \tag{3.12}$$

Here, $\mathbf{G}^{\mathrm{dl}}$ is the Bussgang matrix (2.3) and $\mathbf{d}_k^{\mathrm{dl}}$ is a non-Gaussian quantization distortion uncorrelated with $\mathbf{s}_k^{\mathrm{dl}}$ and its covariance matrix $\mathbf{C}_{\mathrm{d}}^{\mathrm{dl}}$ can be computed in closed-form for the case of $Q = 1$ using arcsine law or approximated for higher resolutions of quantizers according to Section 2.2, where the covariance of the input to the quantizer is $\mathbf{C}_{\mathbf{z}}^{\mathrm{dl}} = \mathbf{PP}^{\mathrm{H}}$.

Assuming that the uth UE has access to its effective channel gain $\left([\mathbf{H}^{\mathrm{T}}\mathbf{G}^{\mathrm{dl}}\mathbf{P}]_{u,u}\right)$, it can estimate its intended stream as $\hat{s}_{u,k}^{\mathrm{dl}} = \left([\mathbf{H}^{\mathrm{T}}\mathbf{G}^{\mathrm{dl}}\mathbf{P}]_{u,u}\right)^{-1} y_{u,k}^{\mathrm{dl}}$.

Similar to the uplink, the ergodic sum-rate can be lower bounded by

$$R_{\mathrm{sum}}^{\mathrm{dl}} = \mathbb{E}_{\mathbf{H}}\left[\sum_{u=1}^{U} \log(1 + \gamma_u^{\mathrm{dl}})\right], \tag{3.13}$$

where γ_u^{dl} is the received SINDR at the uth UE, given by

$$\gamma_u^{\mathrm{dl}} = \frac{|\mathbf{h}_u^{\mathrm{T}}\mathbf{G}^{\mathrm{dl}}\mathbf{p}_u|^2}{\sum_{v \neq u} |\mathbf{h}_u^{\mathrm{T}}\mathbf{G}^{\mathrm{dl}}\mathbf{p}_v|^2 + \mathbf{h}_u^{\mathrm{T}}\mathbf{C}_{\mathrm{d}}^{\mathrm{dl}}\mathbf{h}_u^* + 1} \tag{3.14}$$

The performance of the combiners/precoders mentioned in above will be compared in the following section.

3.3 Channel Model

In this subsection, we review the channel model that we used in Paper B. This channel model will be used to provide simulation results of this chapter. Our focus is on mm-wave propagation in which, the wireless channel is sparse in angular domain, meaning that the behavior of the channel can be represented by the superposition of a small number of paths. A widely-used channel model which is well suited to the sparse characteristic of the mm-wave wireless channels is the clustered channel model [24–26]. In this channel model, N_{cl} clusters of scatterers are considered in which each cluster contributes to N_{ray} of propagation paths. The discrete-time narrow-band multi-user channel impulse response of uplink is $\mathbf{H} = [\mathbf{h}_1, \mathbf{h}_2, ..., \mathbf{h}_U] \in \mathbb{C}^{B \times U}$ where $\mathbf{h}_u$ can be written as

$$\mathbf{h}_u = \sqrt{\frac{1}{N_{\mathrm{cl}}N_{\mathrm{ray}}}} \sum_{n=1}^{N_{\mathrm{cl}}} \sum_{m=1}^{N_{\mathrm{ray}}} \alpha_{n,m}^u \mathbf{a}(\theta_{n,m}^u). \tag{3.15}$$

Here, the fading coefficients $\alpha_{n,m}^u$ are i.i.d. complex random variables drawn from $\mathcal{CN}(0, \sigma_u^2)$ in which σ_u^2 corresponds to the pathloss that the uth UE experiences, $\mathbf{a}(\theta_{n,m}^u)$ is the array response vector of the ULA at the BS in far field in the form of

$$\mathbf{a}(\theta_{n,m}^u) = \left[1, e^{-j2\pi\theta_{n,m}^u}, ..., e^{-j2\pi(B-1)\theta_{n,m}^u}\right]^{\mathrm{T}}, \tag{3.16}$$
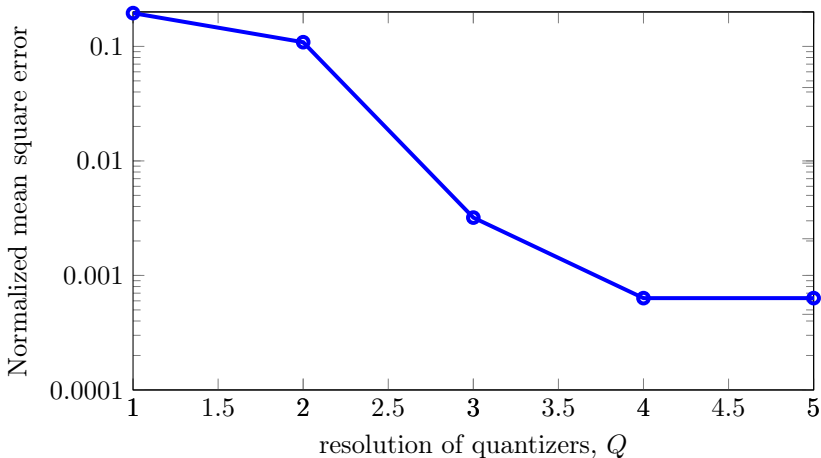
Figure 3.2: Diagonal approximation accuracy for different quantization resolution. The number of antennas

where $\theta_{n,m}^u = d\sin(\phi_{n,m}^u)/\lambda$, d is the antenna spacing, $\phi_{n,m}^u$ is the angle of arrival (AOA) or spatial angle measured from the boresight of the ULA and λ is the wavelength. In the simulation results of this chapter, we consider $N_{\mathrm{cl}} = 2$ and $N_{\mathrm{ray}} = 4$. The pathloss model is chosen as $10\log_{10}\sigma^2(u) = -72 - 29.2\log(d_u)[\mathrm{dB}]$. Shadowing has not been considered in this work. This pathloss model is valid at carrier frequency $f = 28$ GHz [31]. In the next subsection, the performance of the aformentioned combiners and precoders are illustrated using the clustered channel model.

3.4 Simulation Results

3.4.1 Accuracy of the Diagonal Approximation

In Fig. 3.2, the performance of diagonal approximation for different number of bits, Q, is illustrated as the normalized mean square error (NMSE) between the simulated $\mathbf{C_d}$ and $\mathbf{C_d}^{\mathrm{diag}}$. An uplink scenario is considered with clustered channel model according to Section 3.3. The number of antennas is set to $B = 64$, and $U = 8$ UEs are considered. It can be observed that the performance of diagonal approximation is rather poor for single-bit quantization case and improves for larger Q. In the remainder of the thesis, we use arcsine law for $Q = 1$ and diagonal approximation for $Q > 2$.

3.4.2 Study of the Uplink and Downlink Sum Rates

Fig. 3.3 shows the uplink and downlink sum rates for the case of $B = 64$ and $Q = 1$. Three basic combiners and precoders discussed in Section 3.1 and Section 3.2 are

(a) Uplink

(b) Downlink

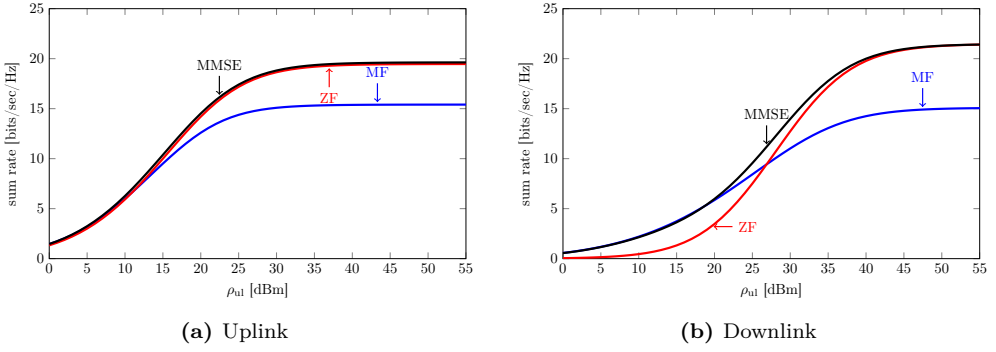**Figure 3.3:** Uplink and downlink ergodic sum rate vs transmit power, B = 64 and Q = 1

considered. As mentioned before, MMSE precoder and DA-MMSE combiner outperform MF and ZF precoder/combiner. Moreover, at low transmit power, the performance of MF approaches that of MMSE/DA-MMSE because of low amount of MUI. At high transmit power, the performance of ZF approaches that of MMSE/DA-MMSE, where AWGN is not dominant anymore.

Summaries of the Appended Papers

In this section, we provide a summary of the two appended papers.

[A] "All-Digital Massive MIMO Uplink and Downlink Rates under a Fronthaul Constraint"

In this paper, we characterize the rate achievable in a bidirectional quasi-static link where several UEs communicate with a massive MIMO BS. In the considered setup, the BS operates in full-digital mode, the physical size of the antenna array is limited, and there exists a rate constraint on the fronthaul interface connecting the (possibly remote) radio head to the digital baseband processing unit. Our analysis enables us to determine the optimal resolution of the analog-to digital and digital-to-analog converters as well as the optimal number of active antenna elements to be used in order to maximize the transmission rate on the bidirectional link, for a given constraint on the outage probability and on the fronthaul rate. We investigate both the case in which perfect channel-state information is available, and the case in which channel-state information is acquired through pilot transmission, and is, hence, imperfect. For the second case, we present a novel rate expression that relies on the generalized mutual-information framework.

[B] "Performance of Quantized Massive MIMO with Fronthaul Rate Constraint over Quasi-Static"

In this paper, we provide a rigorous framework for characterizing and numerically evaluating the error probability achievable in the uplink and downlink of a quantized

MU-MIMO system in a mm-wave quasi-static scenario where the fading channel does not change across the finite-length transmitted codewords, and only imperfect CSI is available at the BS and at the UEs. Moreover, we clarify why standard signal to interference and noise ratio expressions based on ergodic analyses cannot be used in this scenario. We use this framework to study an all-digital massive MIMO system with a fronthaul rate constraint and investigate how the performance in such a system depends on the number of BS antennas and the precision of the analog-to-digital and digital-to-analog converters (ADCs and DACs) and discuss how this trade-off is influenced by the accuracy of the achievable CSI. We adopt a realistic channel model that captures the sparse scattering properties of mm-wave channels, and use an algorithm based on generalized approximate message passing (GAMP), which is able to estimate the channel via uplink pilot transmission, despite the nonlinearity introduced by the finite-precision ADCs. The estimated channel coefficients are used to compute the precoding and combining matrices and to perform mismatched scaled nearest-neighbor decoding. Our non-asymptotic framework captures the cost, in terms of the spectral efficiency, of pilot transmissions - an overhead that the outage capacity, the classic asymptotic metric used in this scenario, cannot capture. We present extensive numerical results that validate the accuracy of the proposed framework and allow us to characterize the optimal number of antennas and the optimal resolutions of the converters, for a given fronthaul rate constraint, to be used in different power regimes and under different CSI assumptions.

Bibliography

[1] Ericsson, "Ericsson mobility report," Nov. 2021.

[2] M. Shafi, A. F. Molisch, P. J. Smith, T. Haustein, P. Zhu, P. De Silva, F. Tufvesson, A. Benjebbour, and G. Wunder, "5G: A tutorial overview of standards, trials, challenges, deployment, and practice," *IEEE J. Sel. Areas Commun.*, vol. 35, no. 6, pp. 1201–1221, 2017.

[3] W. Saad, M. Bennis, and M. Chen, "A vision of 6G wireless systems: Applications, trends, technologies, and open research problems," *IEEE Network*, vol. 34, no. 3, pp. 134–142, 2020.

[4] T. L. Marzetta, "Noncooperative cellular wireless with unlimited numbers of base station antennas," *IEEE Trans. Wireless Commun.*, vol. 9, no. 11, pp. 3590–3600, 2010.

[5] F. Boccardi, R. W. Heath, A. Lozano, T. L. Marzetta, and P. Popovski, "Five disruptive technology directions for 5G," *IEEE Commun. Mag.*, vol. 52, no. 2, pp. 74–80, 2014.

[6] R. W. Heath, N. Gonzalez-Prelcic, S. Rangan, W. Roh, and A. M. Sayeed, "An overview of signal processing techniques for millimeter wave MIMO systems," *IEEE J. Select. Areas Commun.*, vol. 10, no. 3, pp. 436–453, Feb. 2016.

[7] R. H. Walden, "Analog-to-digital converter survey and analysis," *IEEE J. Sel. Areas Commun.*, vol. 17, no. 4, pp. 539–550, 1999.

[8] S. Jacobsson, G. Durisi, M. Coldrey, T. Goldstein, and C. Studer, "Quantized precoding for massive MU-MIMO," *IEEE Trans. Commun.*, vol. 65, no. 11, pp. 4670–4684, Nov. 2017.

[9] S. Jacobsson, G. Durisi, M. Coldrey, U. Gustavsson, and C. Studer, "Throughput analysis of massive MIMO uplink with low-resolution ADCs," *IEEE Trans. Wireless Commun.*, vol. 16, no. 6, pp. 4038–4051, Jun. 2017.

[10] C. Mollén, J. Choi, E. G. Larsson, and R. W. Heath, "Achievable uplink rates for massive MIMO with coarse quantization," in *2017 IEEE International Conference on Acoustics, Speech and Signal Processing (ICASSP)*. IEEE, 2017, pp. 6488–6492.

[11] K. Roth, H. Pirzadeh, A. L. Swindlehurst, and J. A. Nossek, "A comparison of hybrid beamforming and digital beamforming with low-resolution adcs for multiple users and imperfect csi," *IEEE Journal of Selected Topics in Signal Processing*, vol. 12, no. 3, pp. 484–498, 2018.

[12] J. J. Bussgang, "Crosscorrelation functions of amplitude-distorted Gaussian signals," Res. Lab. Elec., Cambridge, MA, Tech. Rep. 216, Mar. 1952.

[13] S. Jacobsson, Y. Ettefagh, G. Durisi, and C. Studer, "All-digital massive MIMO with a fronthaul constraint," in *Proc. IEEE Statistical Sig. Pro. Workshop*, Friburg, Germany, Jun. 2018.

[14] S. Jacobsson, G. Durisi, M. Coldrey, and C. Studer, "Linear precoding with low-resolution DACs for massive MU-MIMO-OFDM downlink," *IEEE Trans. Wireless Commun.*, vol. 18, no. 3, pp. 1595–1609, Mar. 2019.

[15] A. Mezghani and J. A. Nossek, "Capacity lower bound of MIMO channels with output quantization and correlated noise," in *Proc. IEEE Int. Symp. Inf. Theory*, 2012, pp. 1–5.

[16] M. D. McDonnell, N. G. Stocks, C. E. M. Pearce, and D. Abbo, *Stochastic Resonance - From Suprathreshold Stochastic Resonance to Stochastic Signal Quantization*. Cambridge University Press, 2008.

[17] J. Mo, P. Schniter, N. G. Prelcic, and R. W. Heath, "Channel estimation in millimeter wave MIMO systems with one-bit quantization," in *Proc. Asilomar Conf. Signals, Syst., Comput.,*, Pacific Grove, CA, USA, Apr. 2014, pp. 957–961.

[18] O. Dabeer and U. Madhow, "Channel estimation with low-precision analog-to-digital conversion," in *Proc. IEEE Int. Conf. Commun. (ICC)*, 2010, pp. 1–6.

[19] J. Mo and R. W. Heath, "High snr capacity of millimeter wave MIMO systems with one-bit quantization," in *2014 Information Theory and Applications Workshop (ITA)*. IEEE, 2014, pp. 1–5.

[20] F. Rusek, D. Persson, B. K. Lau, E. G. Larsson, T. L. Marzetta, O. Edfors, and F. Tufvesson, "Scaling up MIMO: Opportunities and challenges with very large arrays," *IEEE Signal Process. Mag.*, vol. 30, no. 1, pp. 40–60, 2012.

[21] A. Lapidoth and S. Shamai (Shitz), "Fading channels: How perfect need 'perfect side information' be?" *IEEE Trans. Inf. Theory*, vol. 48, no. 5, pp. 1118–1134, May 2002.

[22] E. Bjornson, L. Sanguinetti, and J. Hoydis, "Can hardware distortion correlation be neglected when analyzing uplink se in massive mimo?" in *2018 IEEE 19th International Workshop on Signal Processing Advances in Wireless Communications (SPAWC).* IEEE, 2018, pp. 1–5.

[23] E. Björnson, L. Sanguinetti, and J. Hoydis, "Hardware distortion correlation has negligible impact on UL massive MIMO spectral efficiency," *IEEE Trans. Commun.*, vol. 67, no. 2, pp. 1085–1098, Feb. 2019.

[24] O. El Ayach, S. Rajagopal, S. Abu-Surra, Z. Pi, and R. W. Heath, "Spatially sparse precoding in millimeter wave MIMO systems," *IEEE Trans. Wireless Commun.*, vol. 13, no. 3, pp. 1499–1513, Mar. 2014.

[25] A. Alkhateeb, O. El Ayach, G. Leus, and R. W. Heath, "Channel estimation and hybrid precoding for millimeter wave cellular systems," *IEEE J. Select. Areas Commun.*, vol. 8, no. 5, pp. 831–846, Jul. 2014.

[26] M. R. Akdeniz, Y. Liu, M. K. Samimi, S. Sun, S. Rangan, T. S. Rappaport, and E. Erkip, "Millimeter wave channel modeling and cellular capacity evaluation," *IEEE J. Select. Areas Commun.*, vol. 32, no. 6, pp. 1164–1179, Jun. 2014.

[27] I. C. Sezgin, M. Dahlgren, T. Eriksson, M. Coldrey, C. Larsson, J. Gustavsson, and C. Fager, "A Low-Complexity Distributed-MIMO Testbed Based on High-Speed Sigma-Delta-Over-Fiber," *IEEE Trans. Microw. Theory Techn.*, vol. 67, no. 7, pp. 2861–2872, Jul. 2019.

[28] S.-H. Park, O. Simeone, O. Sahin, and S. Shamai Shitz, "Fronthaul Compression for Cloud Radio Access Networks: Signal processing advances inspired by network information theory," *IEEE Signal Process. Mag.*, vol. 31, no. 6, pp. 69–79, Nov. 2014.

[29] Y. Li, C. Tao, G. Seco-Granados, A. Mezghani, A. L. Swindlehurst, and L. Liu, "Channel estimation and performance analysis of one-bit massive MIMO systems," *IEEE Trans. Signal Process.*, vol. 65, no. 15, pp. 4075–4089, Aug. 2017.

[30] C. Mollén, J. Choi, E. G. Larsson, and R. W. Heath, "Uplink performance of wideband massive MIMO with one-bit ADCs," *IEEE Trans. Wireless Commun.*, vol. 16, no. 1, pp. 87–100, Jan. 2017.

[31] C. Studer and G. Durisi, "Quantized massive MU-MIMO-OFDM uplink," *IEEE Trans. Commun.*, vol. 64, no. 6, pp. 2387–2399, Jun. 2016.

[32] E. Biglieri, J. G. Proakis, and S. Shamai (Shitz), "Fading channels: Information-theoretic and communications aspects," *IEEE Trans. Inf. Theory*, vol. 44, no. 6, pp. 2619–2692, Oct. 1998.

[33] J. H. Van Vleck and D. Middleton, "The spectrum of clipped noise," *Proc. IEEE*, vol. 54, no. 1, pp. 2–19, Jan. 1966.

[34] L. Lu, G. Y. Li, A. L. Swindlehurst, A. Ashikhmin, and R. Zhang, "An overview of massive MIMO: Benefits and challenges," vol. 8, no. 5, pp. 742–758, April 2014.

[35] Y. Li, C. Tao, A. L. Swindlehurst, A. Mezghani, and L. Liu, "Downlink achievable rate analysis in massive MIMO systems with one-bit dacs," *IEEE Commun. Lett.*, vol. 21, no. 7, pp. 1669–1672, Mar. 2017.

[36] A. K. Saxena, I. Fijalkow, and A. L. Swindlehurst, "Analysis of one-bit quantized precoding for the multiuser massive MIMO downlink," *IEEE Trans. Signal Processing*, vol. 65, no. 17, pp. 4624–4634, Jun. 2017.

[37] J. Mo, P. Schniter, and R. W. Heath, "Channel estimation in broadband millimeter wave MIMO systems with few-bit ADCs," *IEEE Trans. Signal Processing*, vol. 66, no. 5, pp. 1141–1154, Mar. 2017.

[38] J. Östman, A. Lancho, G. Durisi, and L. Sanguinetti, "URLLC with massive MIMO: Analysis and design at finite blocklength," *IEEE Trans. Wireless Commun.*, vol. 20, no. 10, pp. 6387–6401, Apr. 2021.

[39] E. Björnson, J. Hoydis, and L. Sanguinetti, "Massive MIMO networks: Spectral, energy, and hardware efficiency," *Found. Trends Signal Process.*, vol. 11, no. 3-4, pp. 154–655, 2017.

[40] Y. Polyanskiy, H. V. Poor, and S. Verdú, "Channel coding rate in the finite block-length regime," *IEEE Trans. Inform. Theory*, vol. 56, no. 5, pp. 2307–2359, Apr. 2010.

[41] W. Feller, *An Introduction to Probability Theory and its Applications*, 2nd ed., New York, NY, USA, 1971, vol. II.

[42] D. Chu, "Polyphase codes with good periodic correlation properties (corresp.)," *IEEE Trans. Inform. Theory*, vol. 18, no. 4, pp. 531–532, Jul. 1972.

[43] Y. Ettefagh, S. Jacobsson, A. Hu, G. Durisi, and C. Studer, "All-digital massive MIMO uplink and downlink rates under a fronthaul constraint," in *Proc. Asilomar Conf. Signals, Syst., Comput.,*, Pacific Grove, CA, USA, Nov. 2019, pp. 416–420.

[44] O. Dabeer and A. Karnik, "Signal parameter estimation using 1-bit dithered quantization," *IEEE Trans. Inform. Theory*, vol. 52, no. 12, pp. 5389–5405, Dec. 2006.